Chapter 1

Flow Control in Microbial Fuel Cells

Chin-Tsan Wang

Additional information is available at the end of the chapter

http://dx.doi.org/10.5772/58346

1. Introduction

1.1. Mass transfer of MFCs

In Microbial Fuel Cells (MFCs), a mass transfer impact might be larger than expected because it not only effects the mass transfer losses (substrate flux [1, 2] and removal of waste [2]), but also effects the activation losses (mediator [3-5]) and the ohmic losses (proton transfer [6]). However, the convection/diffusion of the reactant transport from the bulk (reactant transport), which can be enhanced by increasing the concentration of reactants and the mean flow rate [7], is able to enhance the power density of the MFCs by effective flow control. Now, a common flow control method of utilizing a magnetic stirrer bar/stirring plate was used to mix the solution of anolytes [8-10]. Nonetheless, some superior flow controls by applying a micro-mixer or micro-channel in the MFCs, which can enhance the power performance [11] in the cases of better solution mixing and without extra power supply, will be addressed in this chapter.

2. Using the magnetic stirrer bar

2.1. Different stirring speed strategies [9]

Different stirring speeds (100, 250, 380 rpm) in the anode of photo microbial fuel cells (PMFCs) have been studied by Lan et al., [9], Lan indicated that the internal resistance fell rapidly at 380 rpm and reached a maximum power density of 1.82mW/m^2. Using a high stirring speed (380 rpm) to mix the anolytes not only decreased the competition of microorganisms for delivering the electrons to the surface of the anode electrode, but also reduced the thickness of the mass transfer boundary layer (MTBL) [9]. However, an external power supply needed for the stirrer bar in PMFCs will weaken it at a larger scale of real application in the future.

3. Applying the micro-mixer or micro-channel in MFCs

The effect of the Reynolds number plays an important role in the flow control of the flow channel because it can affect the flow field of the MFC system. The Reynolds number, Re, shown in equation (1) is defined as the ratio of inertial forces to viscous forces [12]:

$$\mathrm{Re} = \frac{\rho V_0 D_0}{\mu} \tag{1}$$

Where ϱ is the density of fluid, V_0 means the average velocity of inlet flow channel, D_0 is the inlet width of flow channel and μ is the fluid dynamic viscosity coefficient.

In addition, the flow channel is designed to reduce the mass transfer losses of the MFCs. Generally speaking, a higher flow mixing is, the better the power performance of a MFC will be. Therefore, the mixing efficiency, $\varepsilon_{mixing,}$ defined in equation (2) will be used and necessary to identify whether a reactant is uniformly mixed with the anolyte [13]:

$$\varepsilon_{mixing} = 1 - \frac{1}{L}\int_0^L \left| \frac{X_{Ax,outlet} - 0.5}{X_{Amax} - 0.5} \right| dx \tag{2}$$

Where ε_{mixing} is the mixing efficiency, X_{Amax} the maximum concentration of substance A, with the value always set as 1, $X_{Ax,outlet}$ the concentration of substance A at an outlet position, and L is the width of the outlet.

3.1. Convergent flow channel [14]

In this paragraph, a simple flow chamber with a higher flow mixing in MFCs will be addressed. The concept of a convergent flow channel with/without plates (as shown in Fig. 1) applies to the sediment microbial fuel cells (SMFCs) with three Re numbers (Re=30, 60, 90), which have been studied by Wang et al., with Fig. 2 showing the structure diagram of the SMFCs. Compared with a traditional MFC (without channel), the MFC with the convergent flow channel can produce two flow mechanisms (convection and vortex formed, as shown in Fig. 3 and Fig. 4) to enhance the mass transfer, cause the two flow mechanisms to make the substrate move tensely and the mixing more uniform. The electron produced and Hydrogen ion (H^+) will move faster and more actively to reach their objective, which can reduce the mass transfer losses and enhance the electricity production. On the other hand, the performance of a MFC with plates seems to be much more stable than in the case of without plates, causing the vortex flow to limit the moving scale of the substrate and make the transfer speed of the electrons and H^+more uniform, which can thus stabilize the power generation. However, the reason why the existing flow with plates lowers the open circuit voltage (OCV) and the power density has not been clarified clearly, but the other two vortexes (as shown in Fig. 3) caused by the flow plates may prevent some particles from escaping from the vortex scale and cause fewer electrons and H^+participating in the solution.

http://dx.doi.org/10.5772/58346

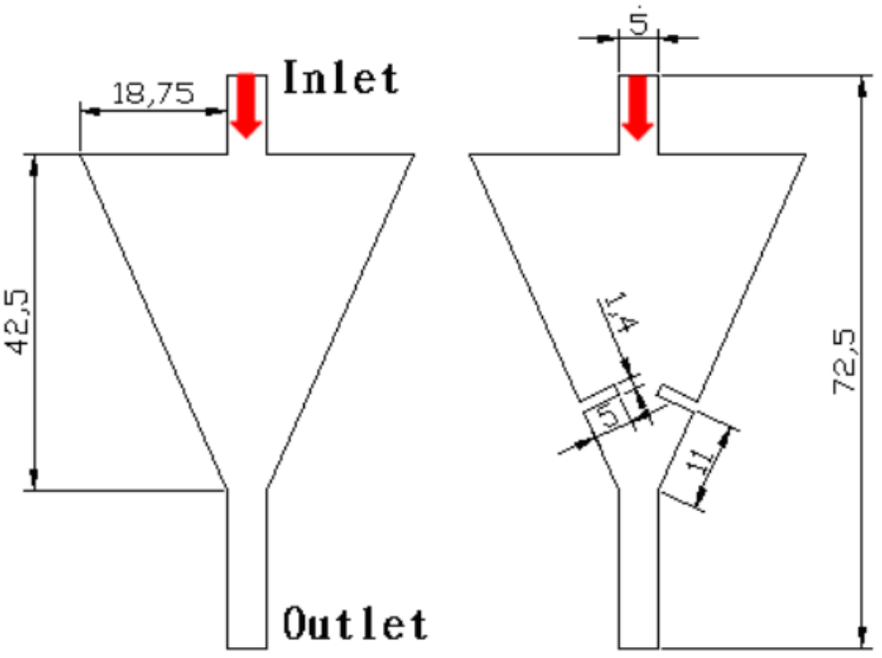

Figure 1. Schematic diagram of convergent flow channel [14].

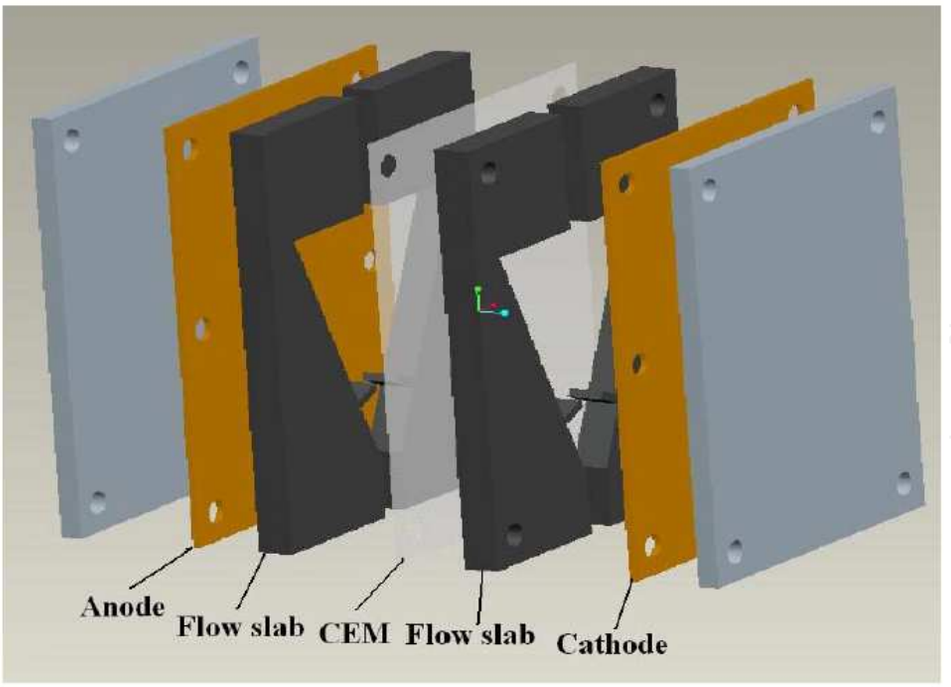

Figure 2. Structure diagram of SMFC [14]

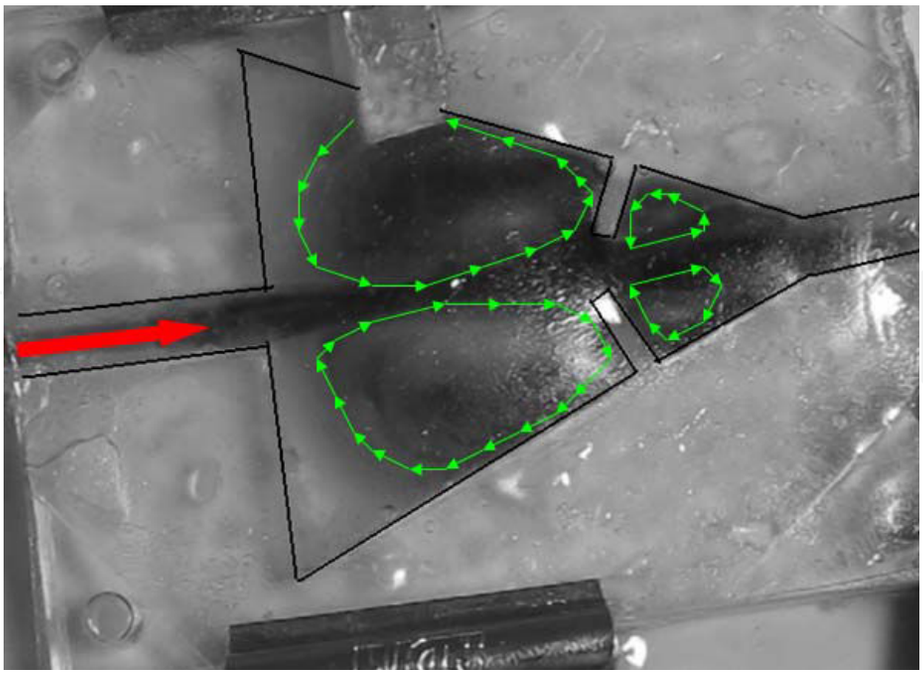

Figure 3. Vortex flow image for convergent flow channel with plates [14]

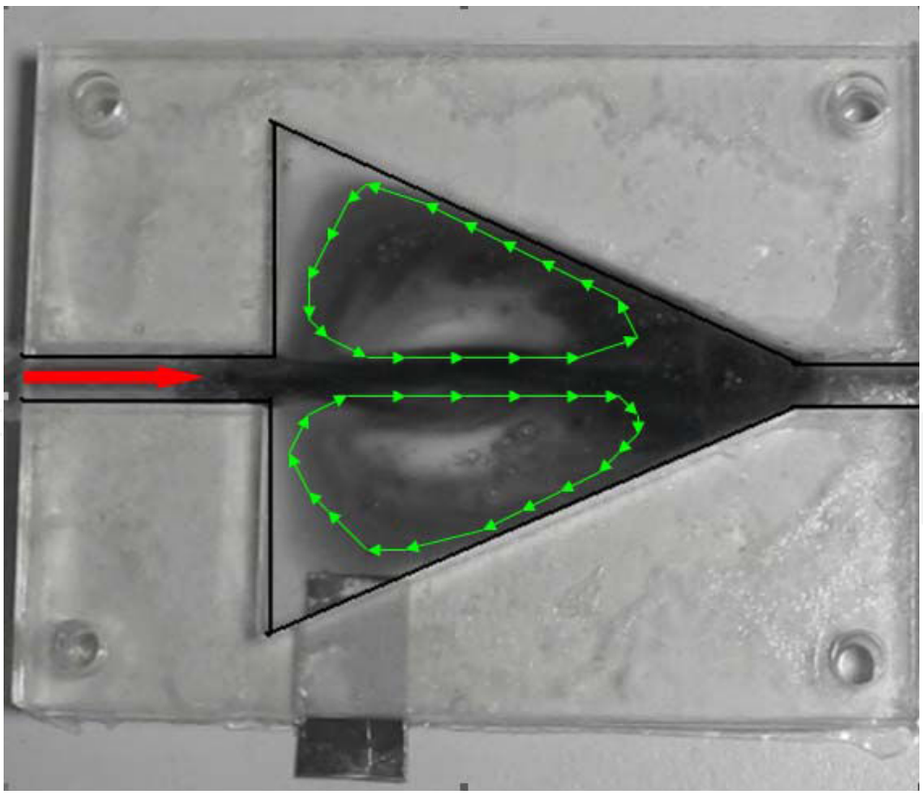

Figure 4. Vortex flow image for convergent flow channel without plates [14]

3.2. Biometric flow channel [15]

Now a biometric concept addressed will be applied in MFCs because the effect of a biometric flow channel (with/without obstacles) on the power generation at different Reynolds numbers (Re=19.85, 496.18), in the single chamber of rumen microbial fuel cells (RMFCs), has been studied by Wang et al.,[15] and the geometrical dimensions and structure of a biometric flow channel can be seen in Figs. 5 and 6.

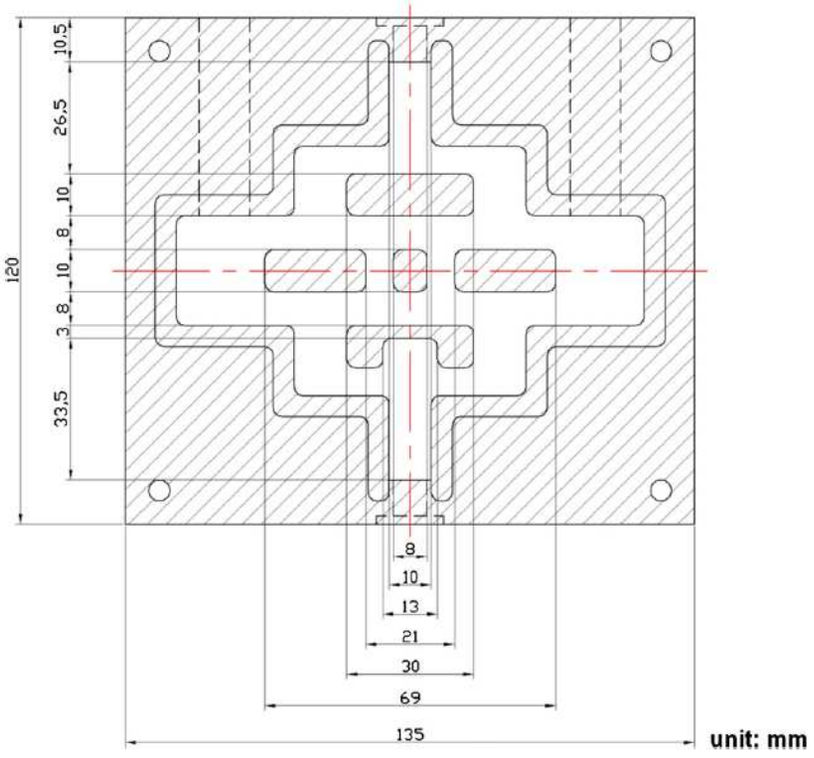

Figure 5. Schematic diagram of biometric flow channel [15].

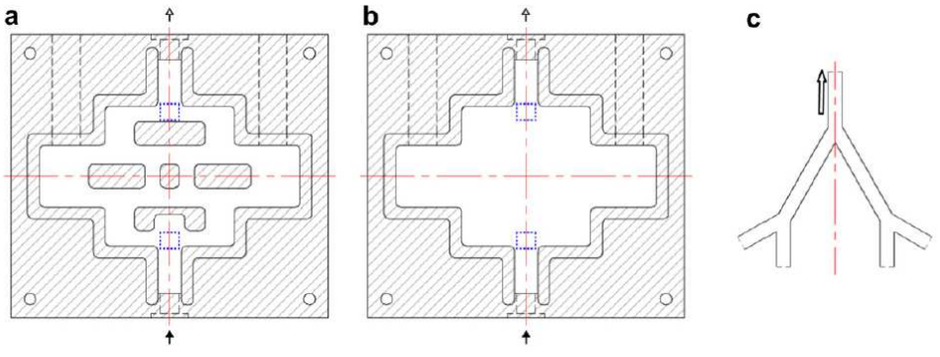

Figure 6. A single chamber (a) with (b) without obstacles marked in the white region for the anode electrode at the bottom of RMFCs [15].

In this study, the simulation result showed that the high flow mixing efficiency obtained by a biometric flow channel with a double two-inlet Y-type inlet channel was above 90%, regardless of being with or without obstacles and different Reynolds numbers. This indicated the mixing mechanism of double two-inlet Y-type inlet channels could greatly enhance the mixing of the reactants before they enter the single chamber of RMFCs.

However, comparing the case of a biometric flow channel without obstacles (No. B/Re=19.85, No. D/Re=496.18), the high Reynolds number [12, 16] and Coanda effect [17] will influence the case of No.D on creating a vortex (as shown in Fig. 7) because it almost did not interact with the main flow and disrupted the reactant atom exchange. Hence, the ohmic and the charge transfer resistance would be increased so that finally some regions of the flow channel based on the need of continuous charging reaction in the fuel cell system would generate a concentration loss. Conversely, the case of No. B would create a smoother flow and a more even reaction at a condition of a lower Reynolds number, thus avoiding concentration loss.

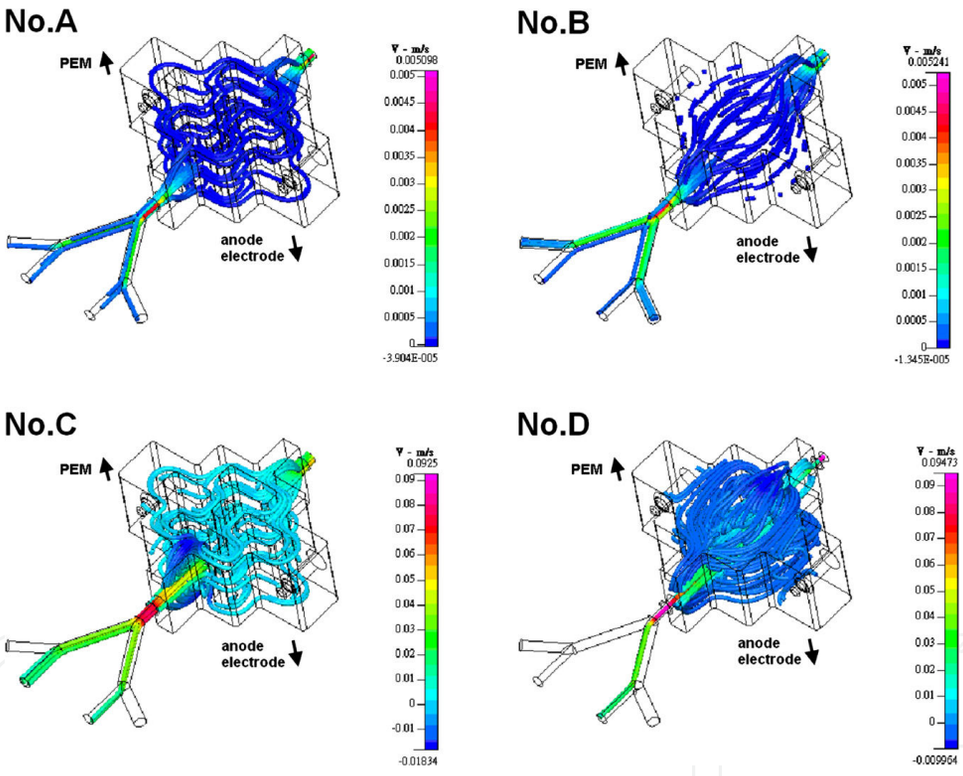

Figure 7. flow velocity images versus different flow conditions and cross-sections analyzed. The location of the anode electrode and proton exchange membranes (PEM) are indicated by arrows [15].

Nevertheless, the flow mixing efficiency of the flow channel in the system was not significantly enhanced by the flow obstacles, but the flow obstacles could evenly distribute the flow field of the reactant [13] on the surfaces of the electrodes and proton exchange membranes. This could avoid concentration loss and also improve power performance [18, 19] along with uneven flow fields. Here, the maximum voltage output and power density in the case of No. C (Re=496.18) would reach 0.716 V and 0.021102 mW/m^2, which is 1.46 times higher than in

the case of No. D 1.08. This result indicated that the flow obstacles of No. C would create a more evenly distributed flow field.

On the other hand, the evidence on decreasing the charge transfer resistance for the RMFCs demonstrated that the biometric flow channels with obstacles indeed improved power performance significantly with a higher Reynolds number, despite an increase in the ohmic resistance. The maximum voltage output and power density showed a positive effect at a higher Reynolds number of Re=496.18 by 2.02 times and 4.09 times more than at the lower Reynolds number of Re=19.85, respectively. This is because the obstacles forced the reactant fluid to have an even flow field [20], thus influencing the microbe to be closer to the anode and proton exchange membrane and so made it easier to create a biofilm.

3.3. Biometric flow channel and biometric mixer[21]

The effect of the biometric flow channel (as shown in Fig. 8) and biometric mixer (as shown in Fig. 9) applied to the MFC has been studied by Wang et al. [21]. Wang indicated that adding the biometric flow channel in the anode chamber could enhance the flow mixing efficiency and the homogeneity of the fluid. Therefore, the maximum power density of a MFC reached 91.81 mW/m^3, which is by far greater than that of a MFC without the biometric channel (1.79×10^{-5} mW/m^3).

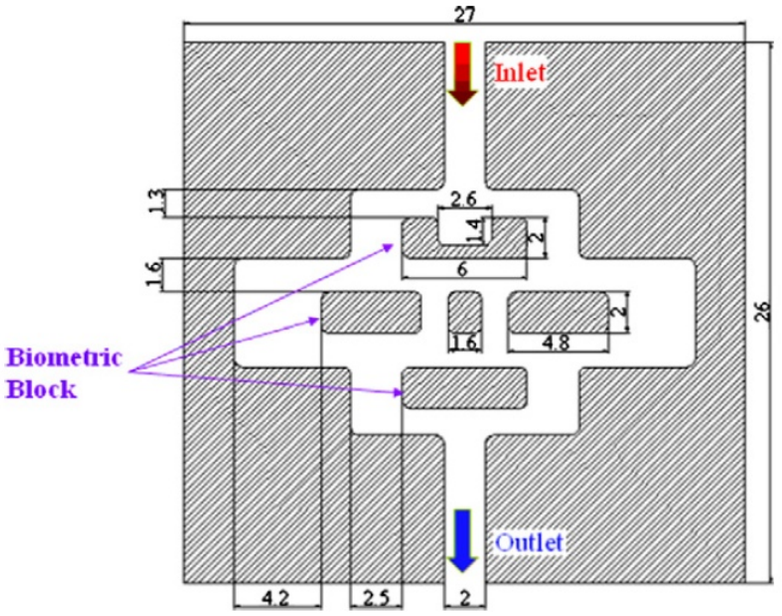

Figure 8. Schematic diagram of the biometric flow channel [21].

The schematic diagram of the biometric flow channel MFC is shown in Fig. 10. However, according to the resulting simulations (as shown in Fig. 11), the biometric mixer generated a high flow mixing efficiency (ε_{mixing}=0.95) of the bacterial liquid and nutrient source before entering the MFC. Then the biometric flow channel enhanced the flow mixing of the reactant

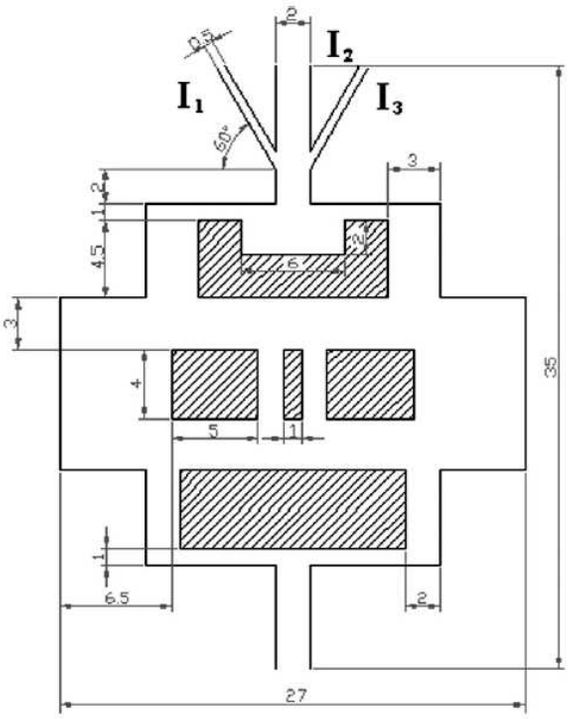

Figure 9. Schematic diagram of the biometric mixer [21].

and a high mixing efficiency of ε_{mixing}=0.98 would be reached at the outlet of the MFC, therefore the maximum power density of the MFC reached 118.34 mW/m^3, which is an improvement of 28.9% compared to the MFC without an added external mixer.

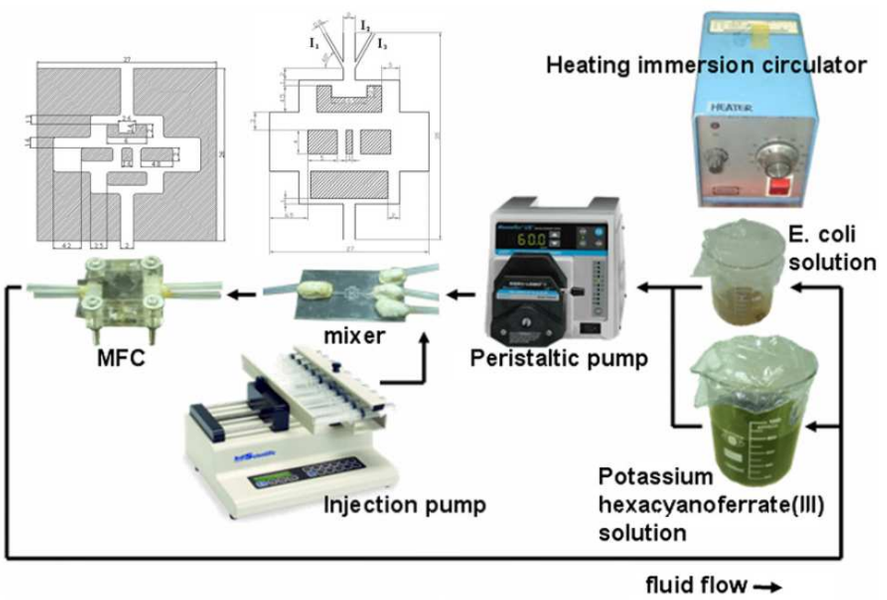

Figure 10. Experimental framework of mixer connected to MFC [21]..

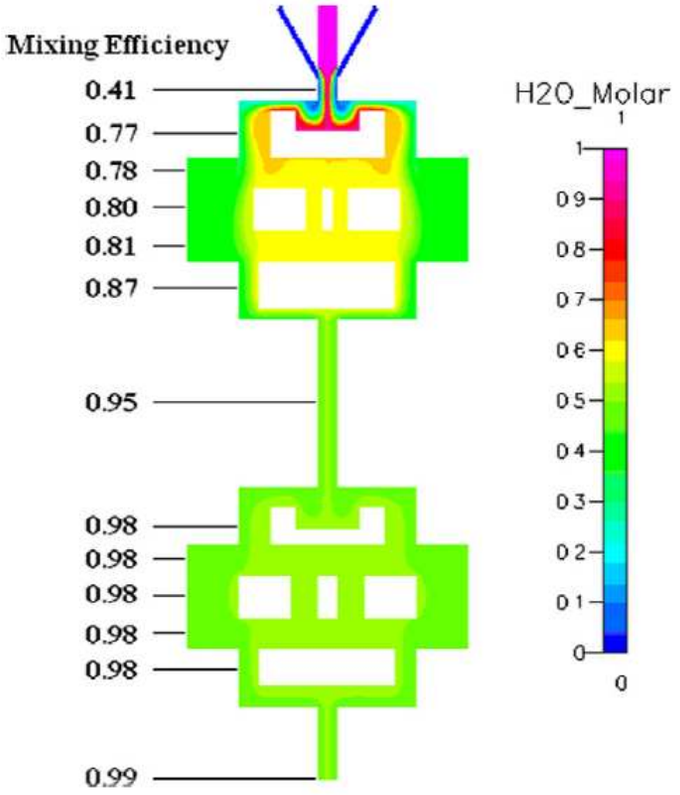

Figure 11. Simulation diagram of mixer connected to a MFC [21]..

3.4. Membraneless microfluidic microbial fuel cell [22]

A membraneless microfluidic microbial fuel cell was used in the Y-shaped microchannel (as shown in Fig. 12), to generate a spontaneous laminar flow on a small scale to separate the cathode and anode to replace the proton exchange membrane [23]. Furthermore, the membraneless microfluidic microbial fuel cell can operate on a short start-up time, with the maximum voltage reached in only 15 min and stable in 45 min at 30 ml/h of flow rate for each stream (as shown in Fig. 12).

As electrical generation of the membraneless μMFC requires a laminar flow with only a little crossover of solute [24]; the Reynolds number (Re) must be less than 10 and the Peclet number (Pe) must be close to 10,000 to maintain the laminar flow and reduce the solute crossover [23]. In this study, the flow rate was increased to 30 ml/h, which reached the maximum open-circuit voltage (OCV) of the membraneless microfluidic microbial fuel cell because the increase in flow rate reduced the diffusion crossover of the solute. Furthermore, the maximum OCV is obtained at Re=8.39 and Pe=7163, which is similar to Choban et al., [23].

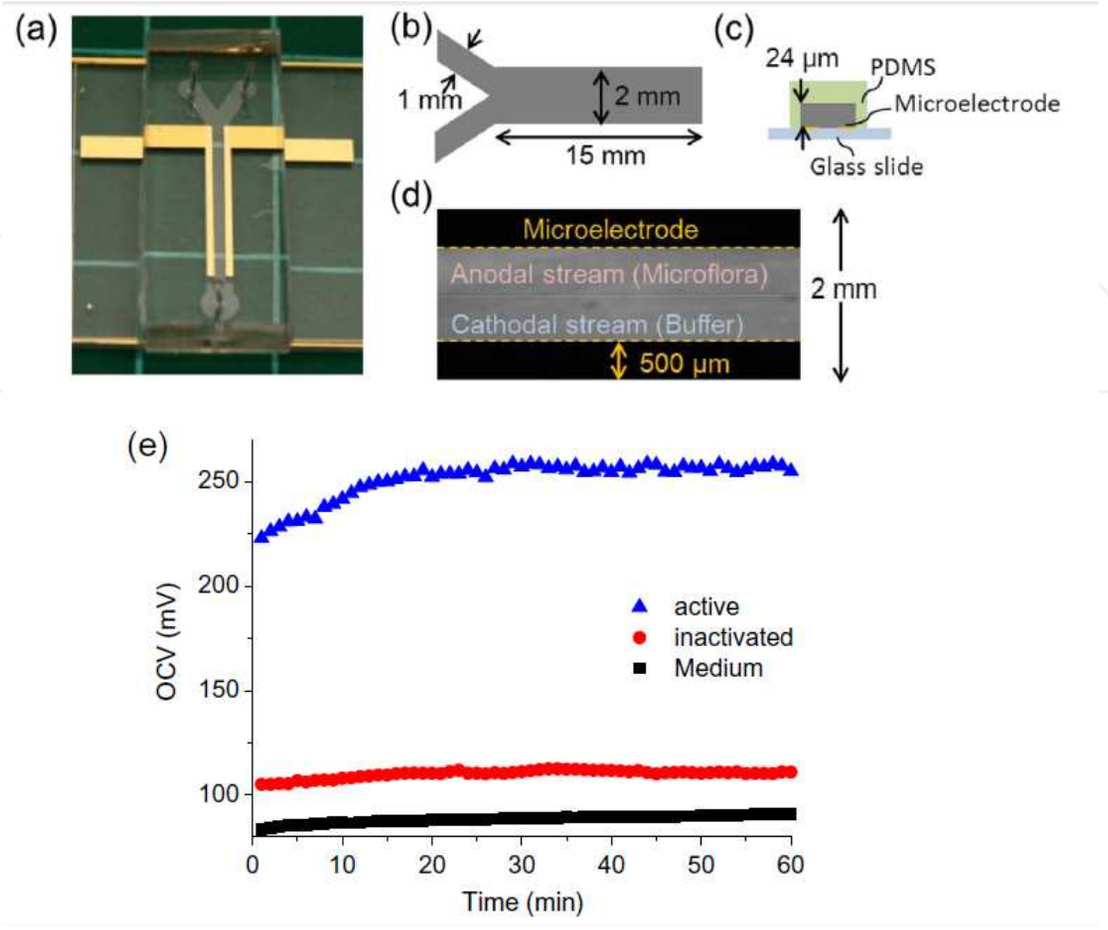

Figure 12. The scheme of the membraneless μMFC and the OCV obtained from the membraneless μMFC [22].

4. Conclusion

Several methods of flow control addressed have been shown to improve the power performance of the microbial fuel cell and can be applied to different applications. A lot of related research has focused on the large scale application, such as wastewater treatment, but a more potential challenge to be considered is a small scale application. The microfluidic microbial fuel cells have the opportunity to be used on biomedical recipients, but the study of the flow control for microbial fuel cells is still limited and there is a need for improvement. Therefore a more sustained research on the method of the flow control, which could be able to improve the practicability of the microbial fuel cell, will be necessary in the future.

Acknowledgements

The author would like to thank the Ph.D candidate of Yan-Ming Chen for his efforts on this chapter.

Author details

Chin-Tsan Wang

National I Lan University, Taiwan

References

[1] Logan BE. Microbial fuel cells. 1st ed., Wiley-Interscience, New Jersey, USA (2008).

[2] He, Z., Minteer, S. D., & Angenent, L. T., Electricity generation from artificial wastewater using an upflow microbial fuel cell, *Environmental science & technology*, *39*(14), 5262 (2005).

[3] Kim, H. J., Park, H. S., Hyun, M. S., Chang, I. S., Kim, M., & Kim, B. H., A mediatorless microbial fuel cell using a metal reducing bacterium, *Shewanella putrefaciens*, *Enzyme and Microbial Technology*, *30*(2), 145 (2002).

[4] Lefebvre, O., Tang, Z., Fung, M. P., Chua, D. H., Chang, I. S., & Ng, H. Y., Electrical performance of low cost cathodes prepared by plasma sputtering deposition in microbial fuel cells, *Biosensors and Bioelectronics*,*31*(1), 164 (2012).

[5] Osman, M. H., Shah, A. A., Wills, R. G. A., & Walsh, F. C., Mathematical modelling of an enzymatic fuel cell with an air-breathing cathode, *Electrochimica Acta*, *112*, 386 (2013).

[6] Kim, J. R., Cheng, S., Oh, S. E., & Logan, B. E., Power generation using different cation, anion, and ultrafiltration membranes in microbial fuel cells, *Environmental science & technology*, *41*(3), 1004 (2007).

[7] Kjeang, E., Djilali, N., and D. Sinton, Microfluidic Fuel Cells: A Review, *J. Power Sources*, 186, 353 (2009).

[8] Liang, P., Huang, X., Fan, M. Z. Cao, X. X., and C. Wang, Composition and Distribution of Internal Resistance in Three Types of Microbial Fuel Cells, *Appl. Microbiol Biotechnol*,77,551(2007).

[9] Raman, K., and J. C. W. Lan, Performance and kinetic study of photo microbial fuel cells (PMFCs) with different electrode distances, *Applied Energy*, 100, 100 (2012).

[10] Oh, S., Min, B., and B. E. Logan, Cathode Performance as a Factor in Electricity Generation in Microbial Fuel Cells, *Environ. Sci. Technol*, 38, 4900 (2004).

[11] Wang, C. T., Shaw, C., K., and T. Y. Hu, Optimization of Flow in Microbial Fuel Cells:An Investigation into Promoting Micro-Mixer Efficiency with Obstacle, *TKJSE*, 14, 25 (2011).

[12] Trirron DJ. Physical fluid dynamics. 2nd ed., Oxford University Inc, New York, USA (1988).

[13] Wang CT, Hu TC, Hu TY. Biophysical micromixer, *Sensor*, 9, 5379 (2009).

[14] Wang, C. T., Fang, S. J., and Z. Q. Qi, Design of Convergent Flow Channel Applied to Sediment Microbial Fuel Cells, *APPEEC*, 1 (2011).

[15] Wang, C. T., Yang, C. M., Chen, Z. S., and T. Shuai, Effect of Biometric Flow Channel on the Power Generation at Different Reynolds numbers in the Single Chamber of Rumem Microbial Fuel Cell (RMFC), Int J Hydrog Energy, 9242 (2011).

[16] Simpson, R. L., Turbulent boundary-layer separation, *Annual Review of Fluid Mechanics*, 21(1), 205 (1989).

[17] Lashkov, Y. A., Sokolova, I. N., & Shumilkina, E. A., Jet flow over ribbed curved surfaces, *Fluid dynamics*, 27(1), 135 (1992).

[18] Logan, B. E., Hamelers, B., Rozendal, R., Schröder, U., Keller, J., Freguia, S.,... & Rabaey, K., Microbial fuel cells: methodology and technology. *Environmental science & technology*, 40(17), 5181 (2006).

[19] Du Z, Li H, Gu T., A state of the art review on microbial fuel cells: a promising technology for wastewater treatment and bio-energy, *Biotech Adv*, 25464 (2007).

[20] Huang, L., Cheng, S., Rezaei, F., & Logan, B. E. Reducing organic loads in wastewater effluents from paper recycling plants using microbial fuel cells. *Environmental technology*, 30(5), 499 (2009).

[21] Qi, Z. Q., Fan, S. J., Wang, C. T., and Z. Y. Hu, Mixing effect of biometric flow channel in microbial fuel cells, *Appl Energ*, 100, 106 (2012).

[22] Wang, H. Y., & Su, J. Y., Membraneless microfluidic microbial fuel cell for rapid detection of electrochemical activity of microorganism, *Bioresource technology*.,145, 217 (2013).

[23] Choban, E.R., Markoski, L.J., Wieckowski, A., Kenis, P.J.A., Microfluidic fuel cell based on laminar flow, J. Power Sources, 128 (1), 54 (2004).

[24] Sprague, I.B., Byun, D., Dutta, P., Effects of reactant crossover and electrode dimensions on the performance of a microfluidic based laminar flow fuel cell.,Electrochimica Acta, 55 (28), 8579 (2010).